Title	Investigation of High-Power Fiber Laser Welding Phenomena of Stainless Steel
Author(s)	Kawahito, Yousuke; Mizutani, Masami; Katayama, Seiji
Citation	Transactions of JWRI. 2007, 36(2), p. 11-15
Version Type	VoR
URL	https://doi.org/10.18910/7955
rights	
Note	

Investigation of High-Power Fiber Laser Welding Phenomena of Stainless Steel †

KAWAHITO Yousuke*, MIZUTANI Masami and KATAYAMA Seiji*****

Abstract

Fiber laser has been receiving great attention due to its advantages of high efficiency, high power and high beam quality, and is expected as one of the most desirable heat sources for high-speed and deep-penetration welding. In this research, therefore, in bead-on-plate welding of Type 304 stainless steel plates with 6 kW fiber laser, the effects of laser power, power density and welding speed on the formation of sound welds were investigated with four laser beams of 130, 200, 360 and 560 μm in spot diameter, and their welding phenomena were explained with high-speed video cameras and X-ray transmission real-time imaging system. The weld beads showed a keyhole type of penetration at all diameters, and the maximum penetration of 11 mm in depth was obtained at 130 μm spot diameter and 0.6 m/min welding speed. It was found that the laser power density exerted a remarkable effect on the increase in weld penetration at higher welding speeds, and sound partially-penetrated welds without welding defects such as porosity, underfilling or humping could be produced at wide process windows of the welding speeds between 4.5 and 10 m/min with fiber laser beams of 360 μm or 560 μm in spot diameter. The high-speed video observation pictures and the X-ray images of the welding phenomena at 6 m/min welding speed and 360 μm spot diameter show that a sound weld bead was formed as a result of the long molten pool suppressing and accommodating spattering and a stable keyhole generating no bubbles from the tip, respectively.

KEY WORDS: (Activating fluxes) (Electron Beam) (Welding)

1. Introduction

Recently, fiber laser has been receiving attention due to its advantages of high efficiency, high power and high beam quality which can produce an ultra-high peak power density of MW/mm^2 levels corresponding to a focused electron beam, and is promising to become one of the desirable heat sources for high-speed and deep-penetration welding [1~7]. Some articles reported that deep-penetration welds could be obtained in stainless steel at high welding speeds [1~3]. However, the effect of laser power density on the formation of sound welds and their welding phenomena were not fully investigated.

In this research, therefore, partial penetration bead-on-plate welding was used on Type 304 stainless steel with a 6 kW high-power fiber laser under several conditions, such as four levels of laser power densities and several welding speeds. Moreover, the typical welding processes were observed with a high-speed video camera or X-ray transmission real-time imaging system in order to clarify the welding phenomena and the mechanisms of welding defects.

2. Experimental Set-Up and Materials Used

The materials used were Type 304 austenitic stainless steel of 8 and 20 mm in plate thickness. 20 mm-thick plates were utilized in cases when a full penetration weld was obtained in an 8 mm-thick SUS304 plate.

A continuous wave (CW) fiber laser (IPG YLR-10000) was used for bead-on-plate welding. The maximum laser power was 10 kW and a beam parameter product (BPP) was 4.5 mm*mrad. The schematic drawing of the experimental set-up for fiber laser welding is shown in **Fig. 1**. A 6 kW-power fiber laser beam was transmitted through two kinds of optical fibers and focused on the specimen surface by lens of two different focusing lengths. Laser beam focusing situations and power density distributions at the focused position are shown in **Fig. 2**, indicating four spot diameters. The fiber laser beams of 130 to 560 μm in spot diameter can produce power densities of 0.6 MW/mm^2 to 20 kW/mm^2. Argon shielding gas was used at the flow rate of 30 *l*/min through an 8 mm-diameter side nozzle. The effect of

† Received on December 14, 2007
* Assistant Professor
** Technical Official
*** Professor

Transactions of JWRI is published by Joining and Welding Research Institute, Osaka University, Ibaraki, Osaka 567-0047, Japan

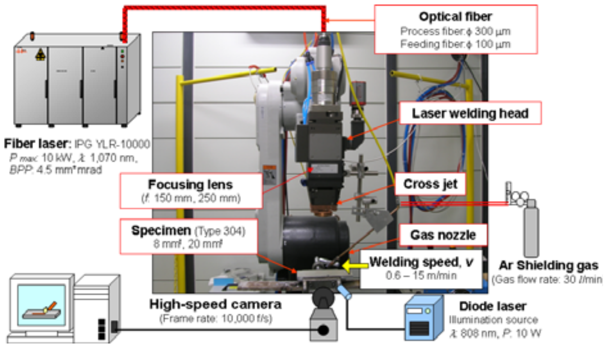

Fig. 1 Schematic experimental set-up for high-power fiber laser welding of Type 304 stainless.

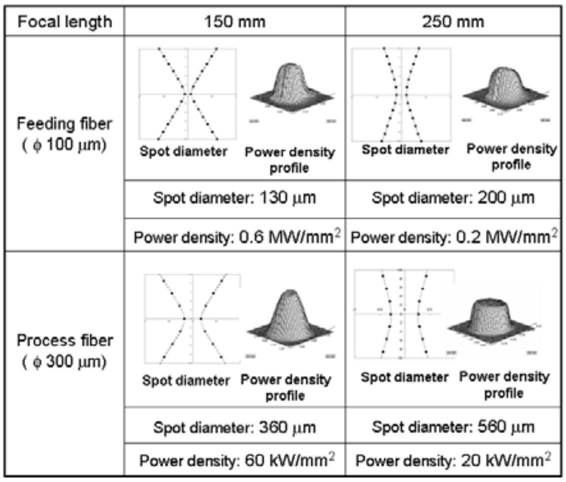

Fig. 2 Fiber laser beam spot diameters, power density and profiles measured with respective fibers and focusing lens.

laser power density on the formation of sound welds was investigated by varying the welding speed.

In order to observe molten pool behavior, a high-speed video camera (Nac: Rx-6) was used at the framing rate of 10,000 f/s with the illumination from a 10 W laser diode (LD) of 808 nm in wavelength and the LD wavelength interference filter for the detailed observation without influence of bright plume emission. In other cases, a xenon arc lamp of 1 kW was also utilized for illumination to observe the whole molten pool. Furthermore, keyhole behavior, bubble formation situation and melt flows inside the molten pool during laser welding were observed at the framing rate of 1,000 f/s through X-ray transmission real-time imaging apparatus as schematically shown in **Fig. 3** [8~10]. Platinum wires of 1 mm in diameter were used to display the geometry of a molten pool during welding and the melt flows inside the molten pool.

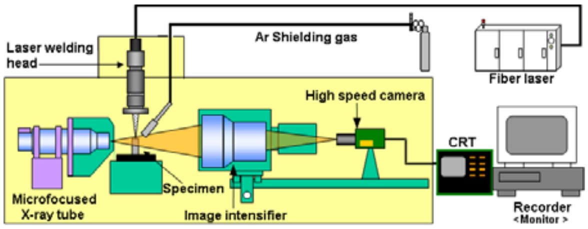

Fig. 3 Schematic drawing of microfocused X-ray transmission in-situ observation system.

3. Experimental Results and Discussion

3.1 Effect of power density on penetration in high-power fiber laser welding

Bead-on-plate welding was performed on Type 304 steel plates with a 6 kW laser beam of 130, 200, 360 or 560 μm spot diameter at several welding speeds of 0.6 to 15 m/min. The typical photos of surface appearances, X-ray inspection images and cross sections of weld beads made at 6 m/min welding speed are shown in **Fig. 4**. Narrow and deep partial-penetration welds could be produced at all spot diameters. The penetration became deeper with a decrease in the laser beam diameter and the consequent increase in the power density, and the maximum penetration was 7.4 mm at 130 μm spot diameter. The surface appearances show that humping was easily formed with the tightly-focused spot diameters of 130 or 200 μm, but according to the X-ray inspection images no pores were generated with lasers beams of all spot diameters.

Subsequently, the surface appearances and cross sections of welds made with the fiber laser beam of a 360 μm-focused spot diameter at the welding speeds of 0.6 to 10 m/min are shown in **Fig. 5**. The weld beads showed a keyhole type of penetration at any welding speeds, and the penetration depths were shallower with an increase in the welding speed. However, porosity was present at less than 3 m/min and underfilled weld beads with spatters were formed at the welding speeds of more than 10 m/min.

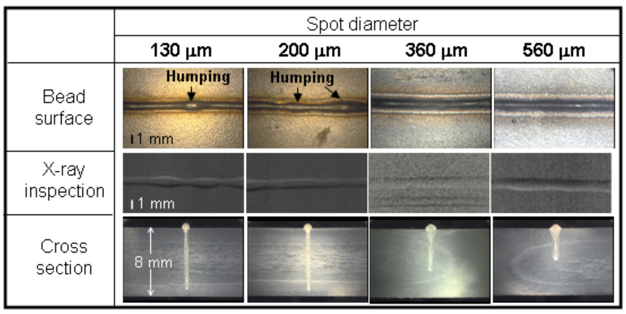

Fig. 4 Surface appearances, X-ray inspection results and cross sections of weld beads produced with 6 kW fiber at various spot diameters.

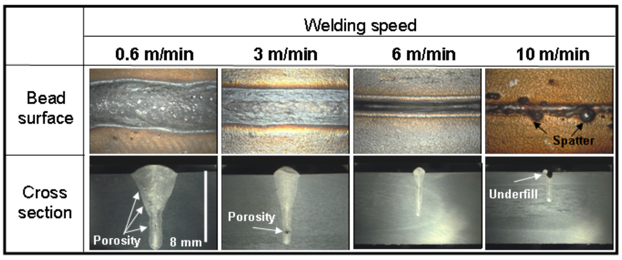

Fig. 5 Surface appearances, X-ray inspection results and cross sections of weld beads produced with 6 kW fiber at various spot diameters.

The weld penetrations made at four spot diameters are plotted as a function of welding speed from 0.6 to 15 m/min in **Fig. 6**. The high laser power density exerted a remarkable effect on the increase in weld penetration at higher welding speeds. The maximum penetration reached 11 mm at 0.6 m/min welding speed and 130 μm spot diameter. However, porosity, underfilling and humping were formed at less than 4.5 m/min welding speeds, at more than10 m/min and with the tightly-focused laser beams of 130 and 200 μm in spot diameter, respectively. As a result, it was found that sound partially-penetrated welds without welding defects could be produced under the wide conditions of welding speeds between 4.5 and 10 m/min with fiber laser beams of 360 μm and 560 μm in spot diameter.

From the above results, it was found that the laser power density exerted a remarkable effect on the increase in weld penetration at higher welding speeds and sound partially-penetrated welds without the welding defects such as porosity, underfilling and humping beads could be produced under a wide range of welding conditions.

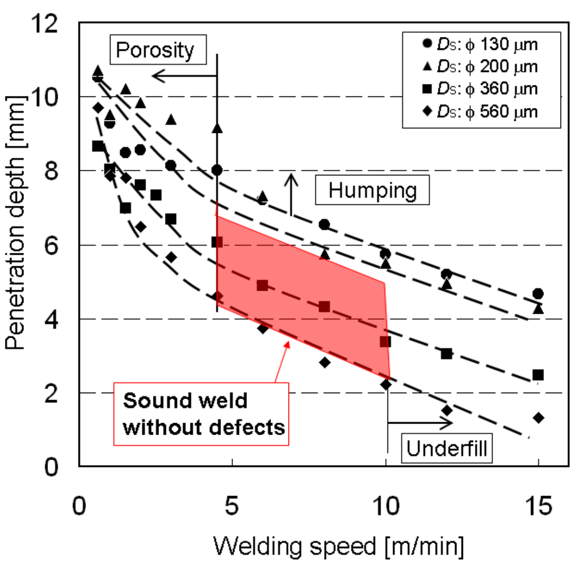

Fig. 6 Effects of fiber laser beam diameter and welding speed on weld penetration and welding defects formation.

3.2 High-speed video observation results of molten pool

Underfilled weld beads with spatters were formed at the welding speeds of 10 m/min or higher in the case of more than 360 μm spot diameter. On the other hand, humping weld beads were produced at the welding speeds of more than 6 m/min with the focused fiber laser beams of 130 and 200 μm in spot diameter.

The high-speed video observation images of the molten pools made with the fiber laser of 360 μm spot diameter at the welding speeds of 6 and 10 m/min are shown in **Fig.** 7(a) and **(b)**, respectively. A LD was used for illumination. At the welding speed of 6 m/min, the molten pool was about 7 mm long along the welding direction. A keyhole was located near the front of the molten pool, the melt flowed out from the keyhole inlet

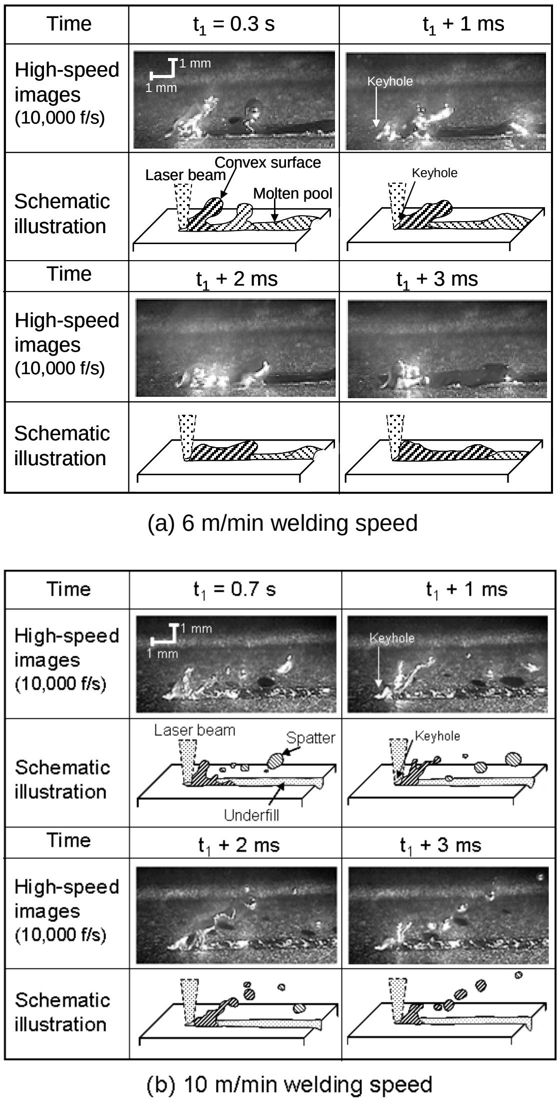

Fig. 7 High-speed video observation results and schematic illustrations of molten surface behavior without or with formation of underfilling and spatters.

to form a convex surface, and the melt sometimes resulted in spatters. However, the long molten pool accommodated the spatter, and produced in sound weld beads. On the other hand, at 10 m/min welding speed, the molten pool became shorter and spattering became more severe, which resulted in underfilled weld beads with spatter. Therefore, it was found that a long molten pool was effective for suppressing and accommodating spattering.

Moreover, the forward or backward welding at 10 degrees along the welding direction at 10 m/min-high-speed was performed in order to reduce underfilling and spattering. The photos of bead surfaces, X-ray inspection results and cross sections of the welds are shown in **Fig. 8**. The bead appearances and cross sections demonstrate that the underfilled weld beads with spatter were greatly improved with the inclined laser beams. No pores were formed according to X-ray inspection photos. However, the penetrations decreased slightly in comparison with the normal irradiation.

Furthermore, **Fig. 9** shows the high-speed video observation images of the molten pool at 130 μm spot diameter and 6 m/min welding speed using a xenon arc lamp illumination. The molten pool had a narrow width of about 2 mm, and a humping part was formed gradually at the rear end of the molten pool. In other words, the humping was not generated at the laser-irradiated position. The humping appears to be caused by superimposed production of melt back-flow accompanied by laser-induced plume and higher surface tension induced by the narrow molten pool width.

From the above results, the high-speed video observation pictures at 6 m/min welding speed showed that a long molten pool was effective for suppressing and accommodating spattering. On the other hand, at 10 m/min higher welding speed the molten pool became shorter and the spattering became more severe, which resulted in underfilling and spattering. The underfilled welds were greatly improved by the laser beam

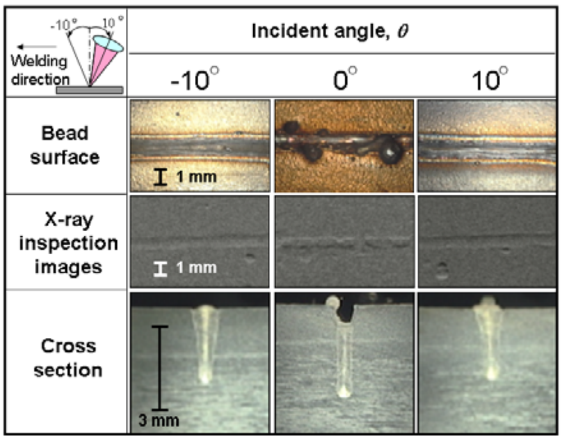

Fig. 8 Effect of inclined laser beam irradiation on formation of underfilling and spatter

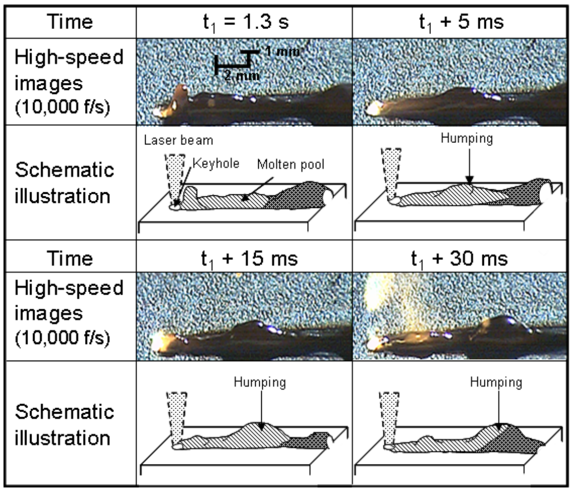

Fig. 9 High-speed video observation results and schematic illustrations of humping weld bead formation at 130 μm spot diameter.

inclination along the welding direction. When using small focused laser beams, humps were periodically formed at the rear end of a molten pool. The mechanism was attributed to superimposed production of melt back flows accompanying laser-induced plume and the high surface tension induced by the narrow molten pool width.

3.3 X-ray in-situ observation results of keyhole behavior and melt flows inside molten pool

A few pores were present at the welding speeds of less than 4.5 m/min, but at the higher speeds pores were absent. X-ray in-situ observation was carried out during welding a Type 304 plate to understand the keyhole behavior, bubble formation and melt flows inside the molten pool. Typical examples of X-ray in-situ observation results with platinum particles under the welding conditions of 6 kW laser power, 360 μm spot diameter, 1.5 and 6 m/min welding speeds are shown in **Fig. 10**. At 1.5 m/min welding speed, strong and fast melt flows were observed from the top to the bottom around the keyhole and from the bottom near the keyhole tip to the rear bottom surface near the solidifying front, which means the existence of the melt flow down the keyhole to the rear surface. On the other hand, the melt at 6 m/min welding speed was observed to flow to the upper along the keyhole wall and then to the rear near the top surface, which was different from that at the low welding speed.

Subsequently, the X-ray images of keyhole behavior and bubble formation situation at the welding speeds of 1.5 and 6 m/min are shown in **Fig. 11**. At 1.5 m/min, bubbles were generated from the tip of the keyhole and then rotated at the bottom part of the molten pool just behind the keyhole. Some bubbles were trapped at the solidifying front of the weld fusion zone, which resulted in porosity. On the other hand, at 6

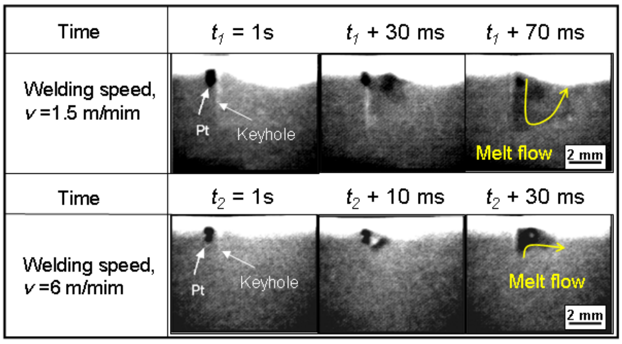

Fig. 10 Microfocused X-ray transmission in-situ observation images of melt flows and molten pool geometry at low and high welding speeds.

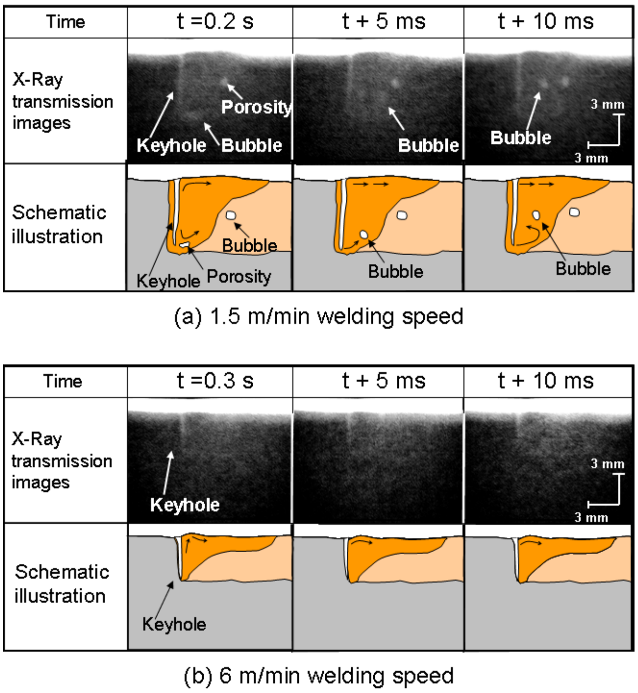

Fig. 11 X-ray transmission in-situ images and schematic illustrations of porosity formation and stable keyhole as well as melt flows and molten pool geometry.

m/min welding speed the keyhole was stable and the bubbles were not formed from the tip of the keyhole, which produced a deeply-penetrated weld bead without porosity.

From the above results, the melts were observed to flow to the upper part along the keyhole wall and then to the rear part near the top surface at the high welding speeds, which was different from those at the low welding speeds. Moreover, it was revealed at high welding speeds that the keyhole was stable and the bubbles were not generated at the tip of the keyhole, which produced a deeply-penetrated weld bead without porosity.

5. Conclusions

The effect of laser power density on the formation of sound welds with the high-power fiber laser was investigated with four different laser beams of 130, 200, 360 and 560 μm in spot diameter, and their welding phenomena were explained with high-speed video cameras and X-ray transmission real-time imaging system during bead-on-plate welding of SUS304 plates with 6 kW fiber laser. The welds showed a keyhole type of penetration at any diameters and the maximum penetration of 11 mm depth was obtained at 130 μm spot diameter at 0.6 m/min welding speed. Moreover, it was found that the laser power density exerted a remarkable effect on the increase in weld penetration at higher welding speeds, and sound partially-penetrated welds without welding defects such as porosity, underfilling or humping could be produced with fiber laser beams of 360 μm and 560 μm in spot diameter under a wide range of welding conditions at the welding speeds between 4.5 and 10 m/min. The high-speed observation pictures and the X-ray images of the welding phenomena at 360 μm spot diameter and 6 m/min welding speed demonstrated that a sound weld bead was formed owing to a long molten pool suppressing and accommodating spattering, and a stable keyhole generated no bubbles from the tip.

Acknowledgements

This work was conducted as part of the project, "Development Base of Joining Technology for New Metallic Glasses and Inorganic Materials" (DBJT) cooperated by Joining and Welding Research Institute (JWRI) of Osaka University. The authors would like to acknowledge Mr. Keisuke Kinoshita, a graduated student of Mechanical Engineering Course of Osaka University, for his help in some experiments.

References

1) Thomy C, Seefeld T and Vollertsen F 2005 Proc. the Third International WLT-Conference on Lasers in Manufacturing (Munich, Germany) pp.27-32.
2) Vollertsen F and Thomy C 2005 Proc. ICALEO (Miami, USA) pp.254-263.
3) Verhaeghe G and Hilton P 2005 Proc. the Third International WLT-Conference on Lasers in Manufacturing (Munich, Germany) pp.33-38.
4) Verhaeghe G and Hilton P 2005 Proc. ICALEO (Miami, USA) pp.264-271.
5) Kancharla V 2006 Proc. ICALEO (Scottsdale, USA) pp.579-585.
6) Ream S 2006 Proc. ICALEO (Scottsdale, USA) pp.586-594.
7) Liu Z, Kutsuna M and Xu G 2006 Proc. ICALEO (Scottsdale, USA) pp.562-568.
8) Seto N, Katayama S and Matsunawa A 2000 J. of Laser Applications 12 245-250.
9) Naito Y, Mizutani M. and Katayama S 2003 Proc. ICALEO (Jacksonville, USA) Paper ID. 1005.
10) Katayama S, Uchiumi S. and Briand F 2006 Proc. ICALEO (Scottsdale, USA) pp.953-959.